EPFL

Advanced Ceramic Technologies

Grain boundaries: complexions and character

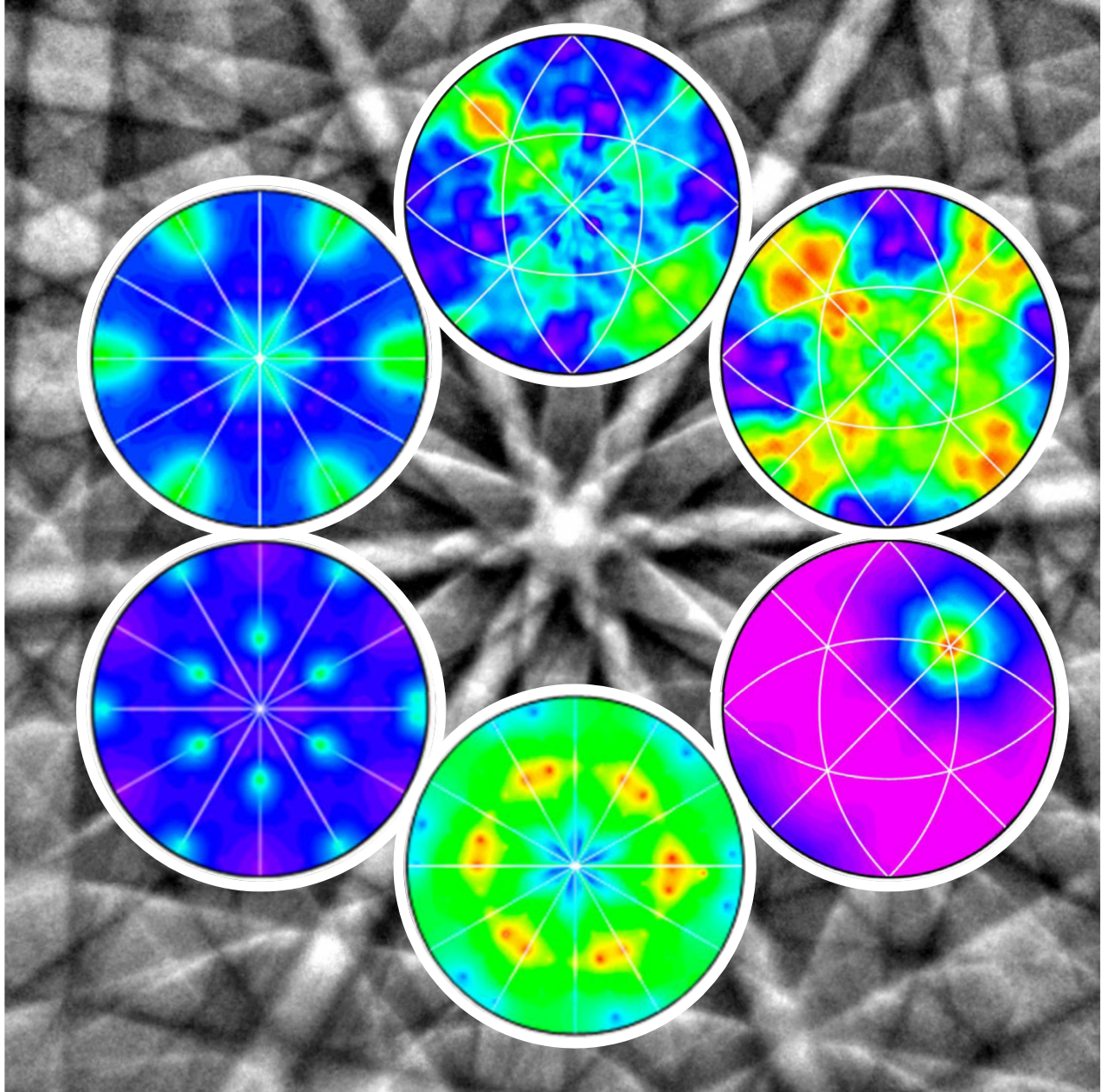

M. Stuer

Outline

- Complexions and complexion transitions
  - Thermodynamic description
  - Role of grain boundary energy and grain growth
- EBSD basics
  - Stereographic projections, pole figures and inverse pole figures
- Stereological EBSD analysis
  - Description of stereological method
- Effect of complexion transitions on grain boundary plane/character distribution

Learning objectives:

- Understand the complexity behind grain boundary engineering (5-geometric, complexions, …)
- Acquire method to investigate grain boundary character distribution in microstructures
- Illustrate direct consequences of complexion transitions

(simplified) Grain boundary descriptors

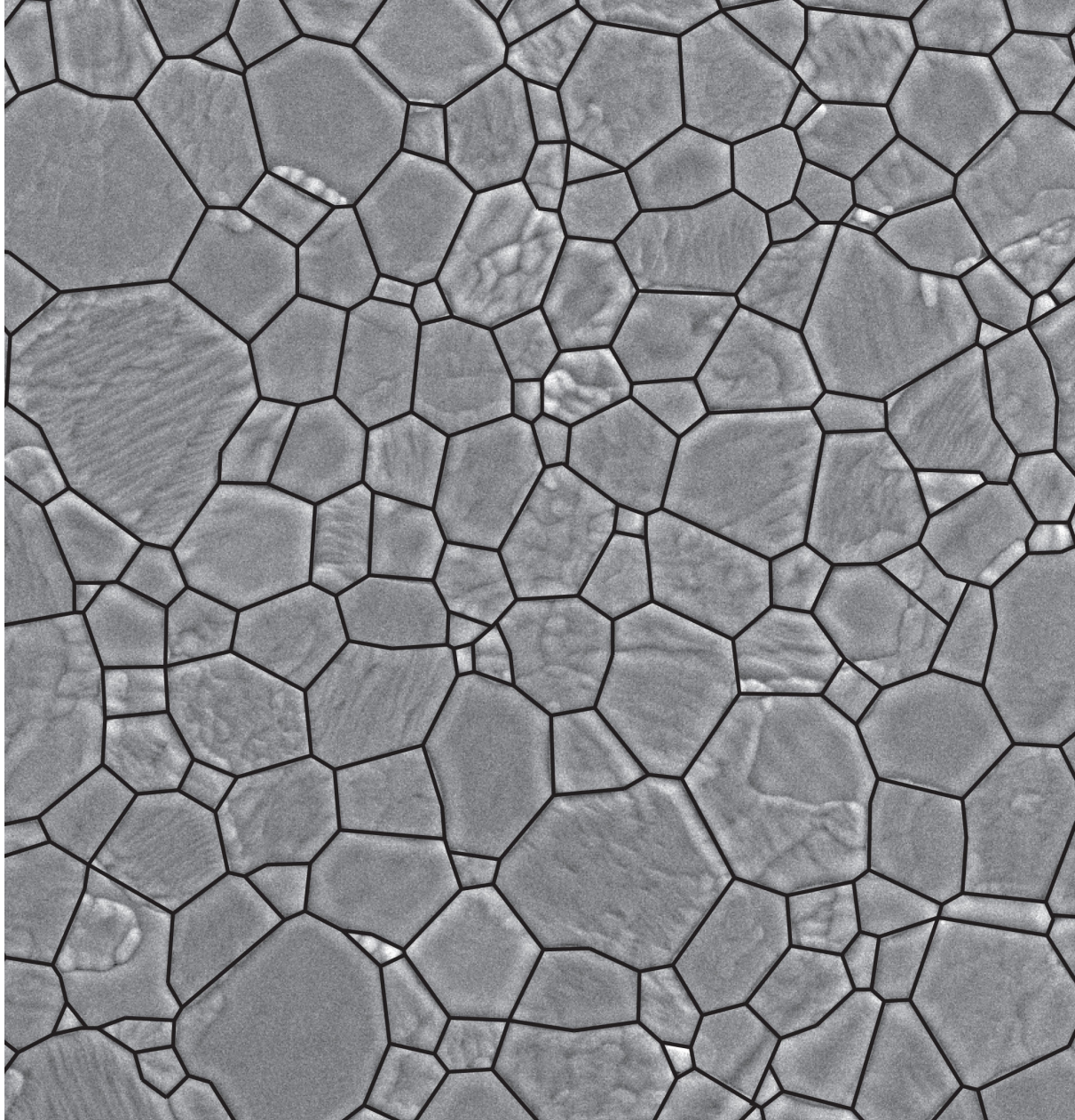

M. Stuer

Grain boundary description methods

- **Geometric** (and structural) description
  - **Twist**: one part of crystal rotated around an axis normal to the boundary plane
  - **Tilt:** one part of crystal twisted around an axis in the boundary plane
- **Misorientation angle** based description
  - Low angle: misorientation < 15° (typically lower energies)
  - High angle: misorientation < 15° (typically higher energies)
- **Coincidence site lattice** (CSL) boundaries
  - Describes degree of lattice matching between two grains
  - Lower Σ values indicate higher atomic coincidence and lower boundary energy (e.g. Σ3 for twin boundaries)
- **Crystallographic description**
  - Based on 5 macroscopic parameters
    ➔ Lattice misorientation + Boundary plane normal

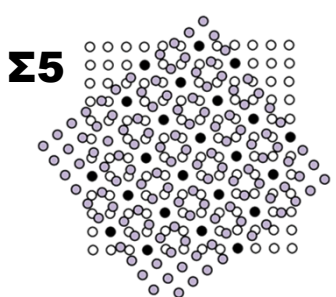

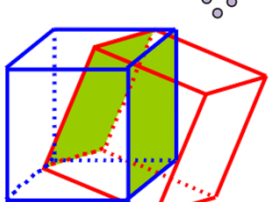

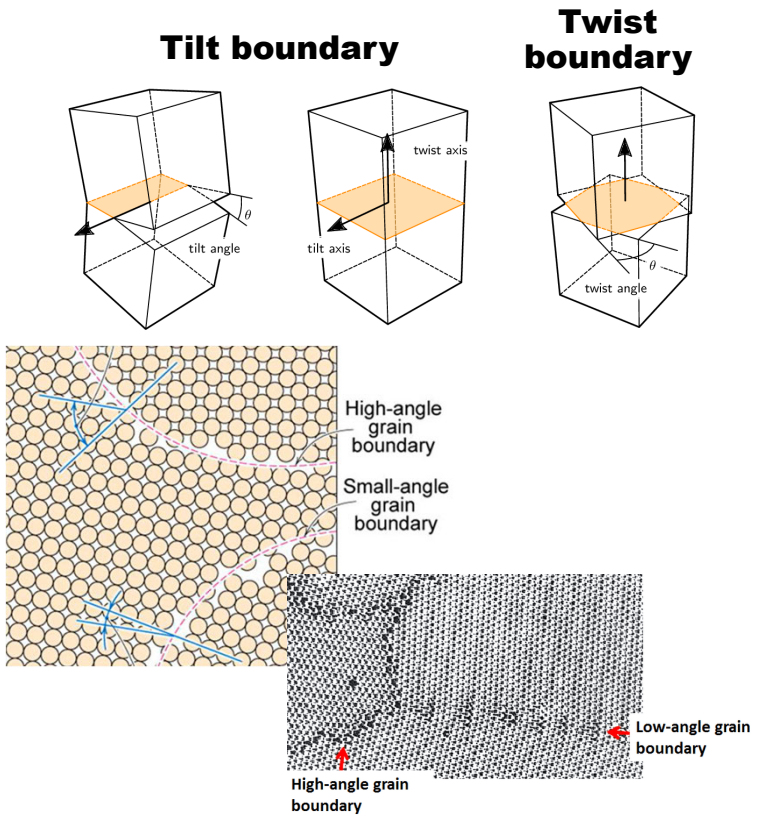

Important to note:

GBs have also distinct atomic and chemical structures

Grain boundaries

Complexions and complexion transitions

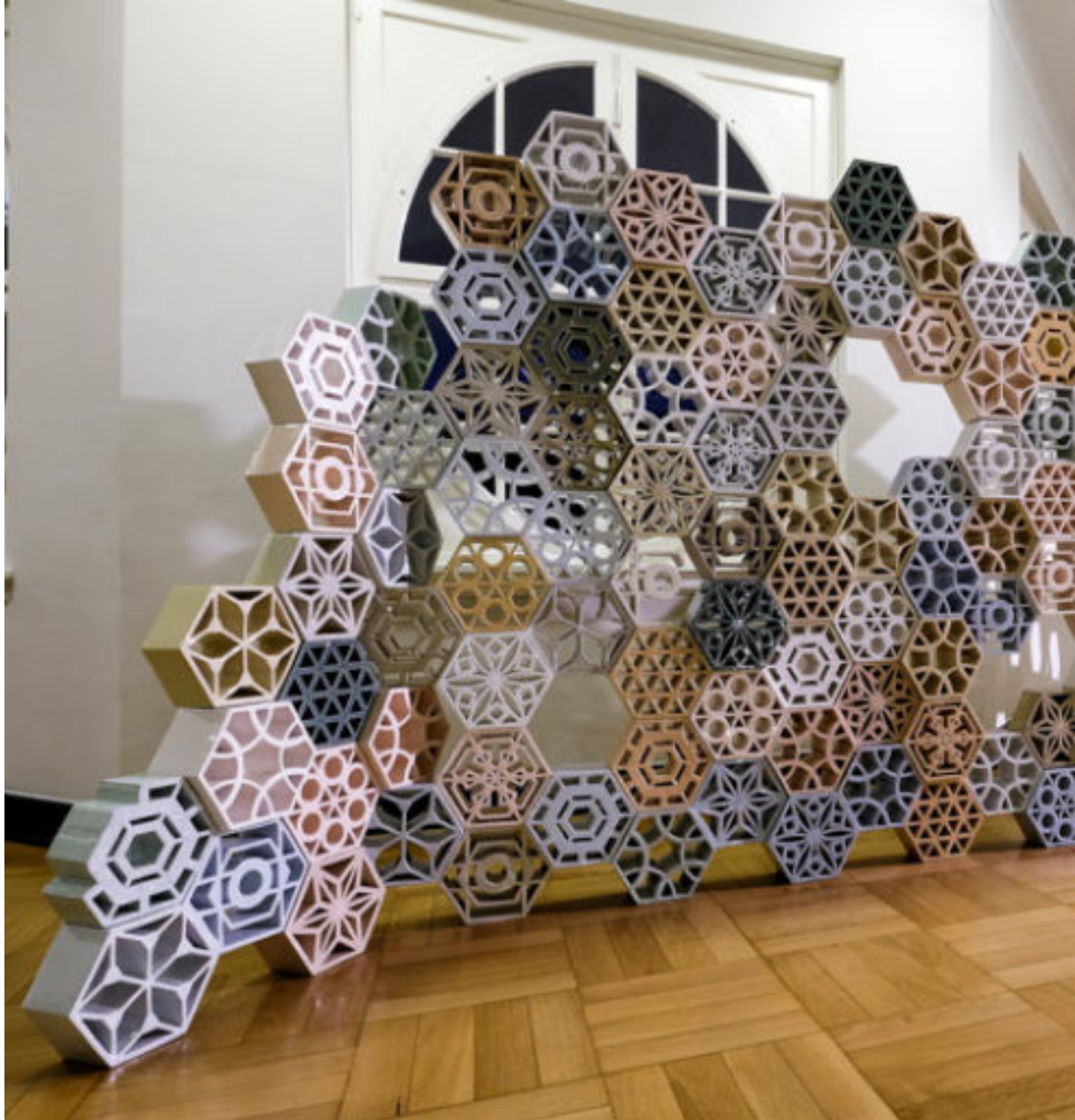

M. Stuer

Basics about complexions and complexion transitions

- Grain boundaries are **not phases**
  - ➔ they **cannot exist independently**
  - ➔ only exist as a result of the adjacent grains
- Grain boundaries can undergo **structural transitions** (similar to phase transitions in bulk)
  - ➔ structures and structure transitions referred to as **complexions and complexion transitions**
- **Minimal description** of GB excess free energy / unit area γ depends on
  - bulk **thermodynamic state variables** (T, P, μ_i)
  - five macroscopic **interface parameters**:
    - 3 for misorientation $\boldsymbol{R}$ between adjacent grains faces
    - 2 for GB plane normal orientation ($\hat{\boldsymbol{n}}$)
- Other parameters exist such as excess of impurities/ dopants and point defects, structural/compositional gradients, microscopic displacement (e.g. disconnections), …

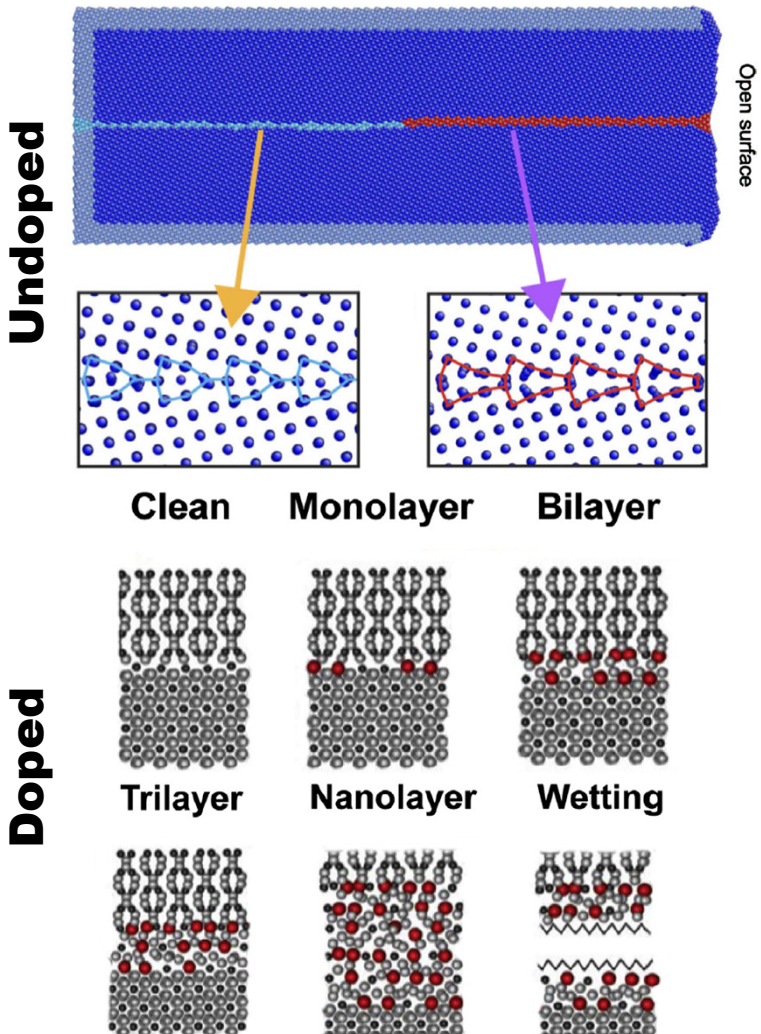

source: 10.1016/j.actamat.2013.07.037

Basics about complexions and complexion transitions

- T, P subspace: **GB adopts complexion** associated **with lowest γ** (e.g. energy) for given T, P
  - GB of complexion type α stable for high P / low T
  - GB of complexion type β stable for high T / low P

  ➔ **Transition** occurs when **energy curves cross**

- Complexion transitions can be:
  - **first order** (γ continuous, $\partial\gamma$ discontinuous)
    ➔ transition occurring on crossing of competing grain boundary free energy curves (e.g. clean to monolayer, …)
  - **second order** ($\partial\gamma$ continuous, $\partial^2\gamma$ discontinuous)
    ➔ gradual replacement of one type of grain boundary repeating structural unit for another (e.g. gradual replacement of GB units)

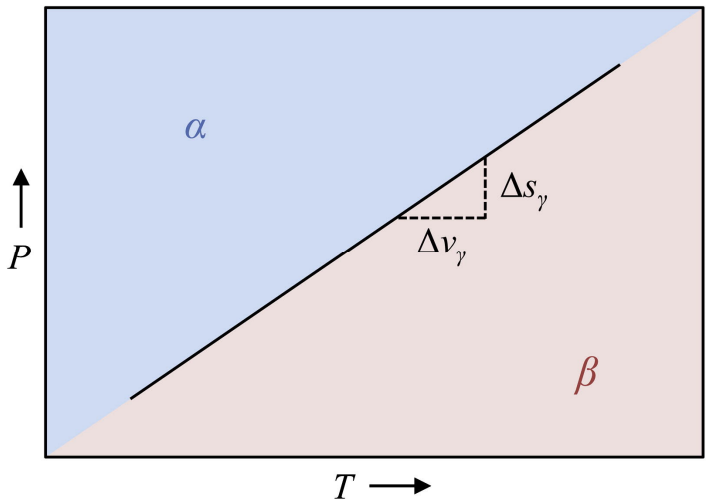

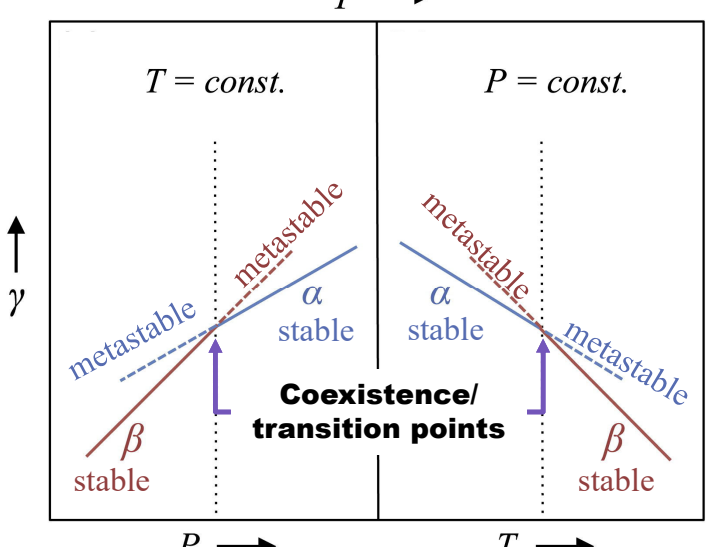

source: 10.1016/j.actamat.2013.07.037

Complexions

Complexion and complexion transitions

- **Coexistence line** between complexions α, β exists and defined by underlying thermodynamics
  - $\Delta\left(\frac{\partial\gamma}{\partial T}\right)_P = -\Delta s_\gamma$ (change in entropy)
  - ➔ **Discontinuity** in first derivative corresponds to **latent heat** ($Q = T\Delta S$) of complexion transition
  - $\Delta\left(\frac{\partial\gamma}{\partial P}\right)_T = -\Delta v_\gamma$ (change in GB volume)
  - ➔ **Discontinuity** in first derivative corresponds to **specific excess GB volume change**
- Proportion (i.e. character distribution) of coexisting complexions determined for example by internal stresses

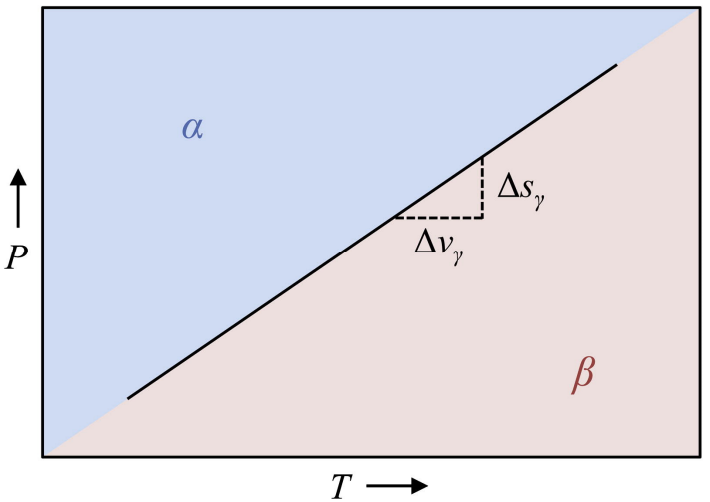

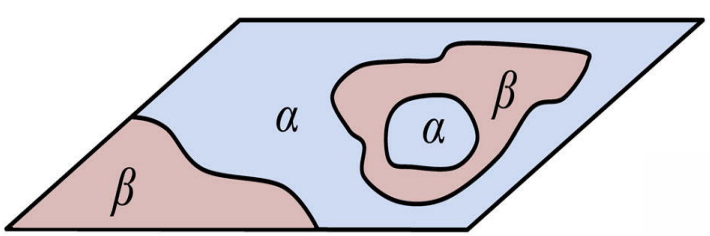

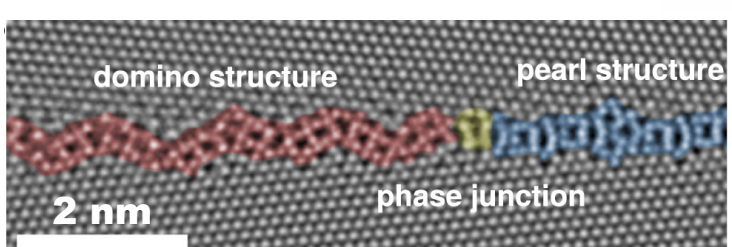

sources: 10.1016/j.actamat.2013.07.037, 10.1038/s41467-022-30922-3

Congruent vs non-congruent complexion transitions

- **Congruent complexion transition**
  GB shape/geometry (misorientation vector $\boldsymbol{R}$ and GB normal $\hat{\boldsymbol{n}}$) do not change during transition
  ➔ 5-parameter GB character remains constant (e.g. transition from monolayer to bilayer)
- **Non-congruent transition:**
  change in geometrical parameters (i.e. 5-parameter GB character)
  - facet formation, where $\hat{\boldsymbol{n}}$ splits into components $\hat{\boldsymbol{n}}_1$ and $\hat{\boldsymbol{n}}_2$ whose weighted average is $\hat{\boldsymbol{n}}$
  - dissociation into two new interfaces separated by a wetting layer, which may be crystalline with well-defined misorientations $\boldsymbol{R}_{1,2}$ whose sum is $\boldsymbol{R}$, or non-crystalline where the original $\boldsymbol{R}$ is maintained across the spatial gap

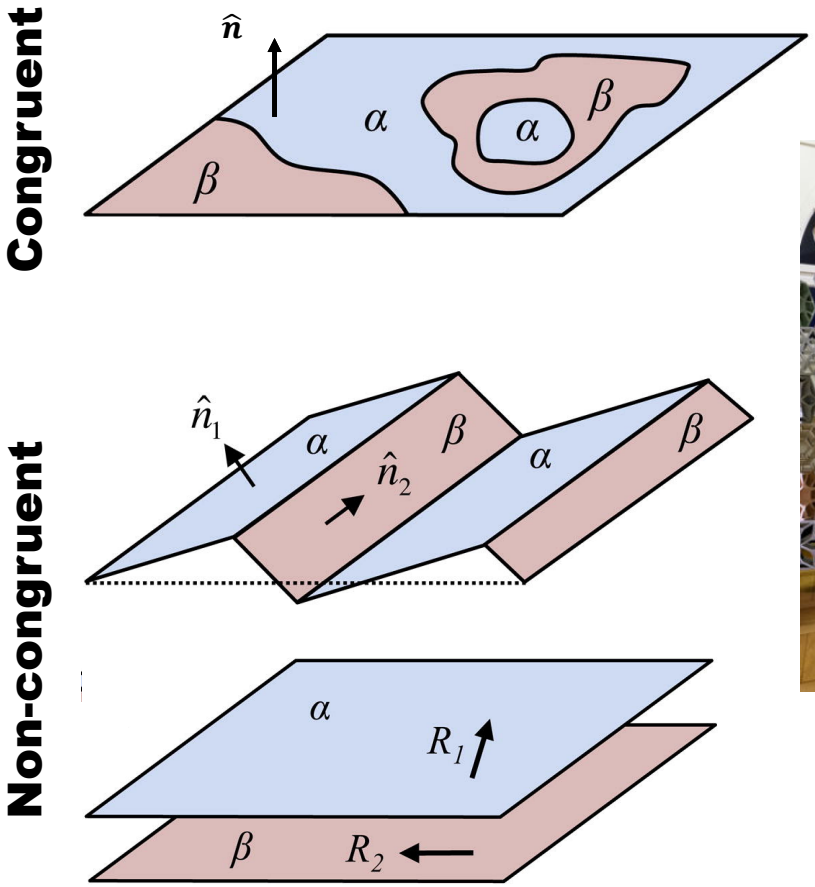

Complexions

source: 10.1016/j.actamat.2013.07.037

Thermodynamic description of complexion transitions

- Though **complexion transitions** are referred to as structural GB changes, they may involve **chemical composition changes in addition to structural rearrangement**

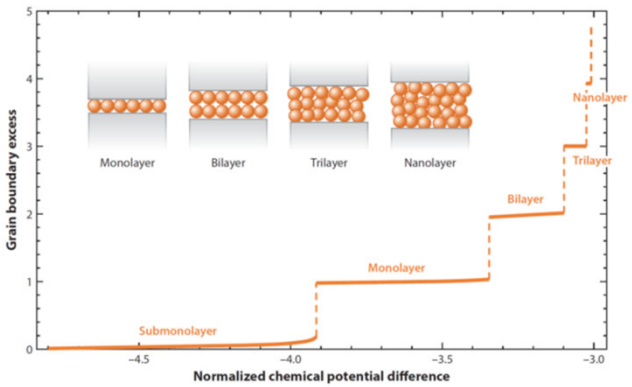

- **Grain boundary energy change** described as:

$$d\gamma = -[S]_{N_1} dT - [V]_{N_1} dP - \sum_{i=2}^{C} [N_i]_{N_1} d\mu_i$$

- $[S]$ excess entropy
- $[V]$ excess volume
- $[N_i]$ excess of component i at interface
- T temperature
- P pressure
- μ chemical potential

- Complexion transitions lead to **discontinuous property changes** (e.g. GB mobility, GB energy, diffusivity,…)
  - ➔ Observation of discontinuous change in characteristics (e.g. GB mobility) indicator of complexion transition

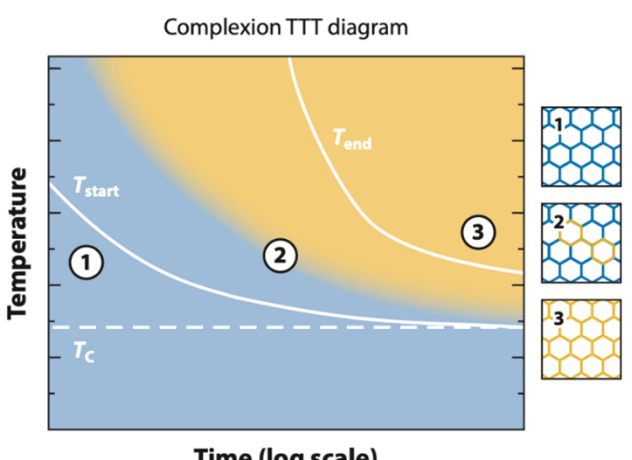

- **Note:**
  Transition points are **specific to complexions themselves** (e.g. each complexion has its own)
  - ➔ Rapidity of change (and thus detectability) depends on proportion within material!

Congruent complexion examples

- **First order** (i.e. discontinuity in composition) complexion transitions observed in alumina
  - **Six discrete** ”Dillon-Harmer” **complexions** (type I to VI)
  - GB thickness not arbitrary but rather determined by thermodynamic equilibrium conditions
- **Grain boundary mobilities** found to **increase with complexion thickness** from type I to type VI

Note:
Proof of existence of mobility increasing complexion transitions, does not per se negate the opposite!

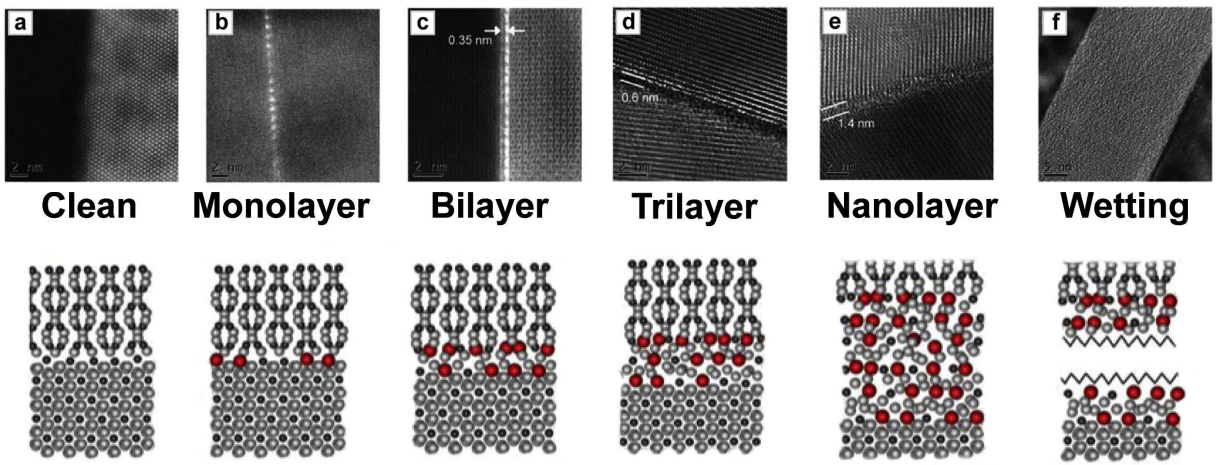

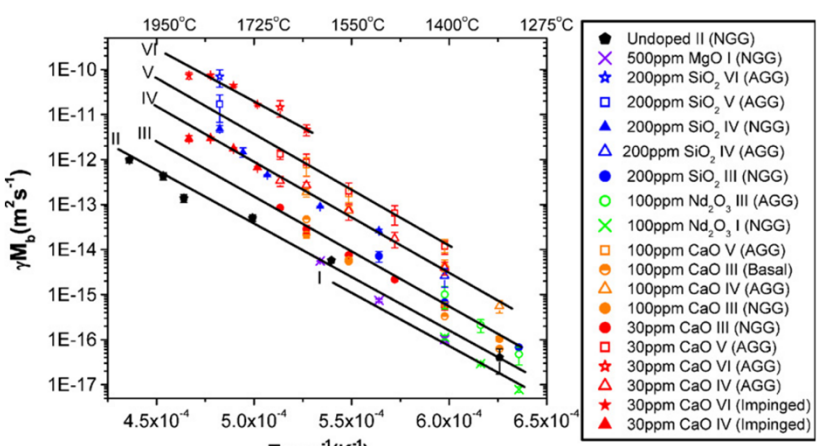

source: 10.1016/j.actamat.2013.07.037

Grain boundary energies and complexion transitions

- **Thermal grooving** of a polished surface followed by atomic force microscopy allows determining the **grain boundary energies**:

$$\gamma_{GB}/\gamma_S = 2\cos(\Psi_S/2)$$

  ➔ **Higher dihedral angles** Ψ_S represent **lower grain boundary energies** and vice-versa

- **Complexion transitions** effectively reduce grain boundary energies
  ➔ Upon complexion transition occurrence **average grain boundary energy decreases**

- **Grain growth** due to higher grain boundary mobility keeps forming **new grain boundaries**
  ➔ Range of grain boundary energy distribution remains similar
  ➔ Since complexion transitions reduce GB energy, **new GBs with high energy** must be **continuously formed**

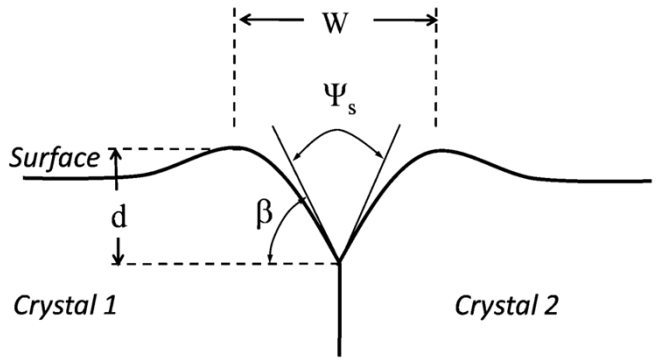

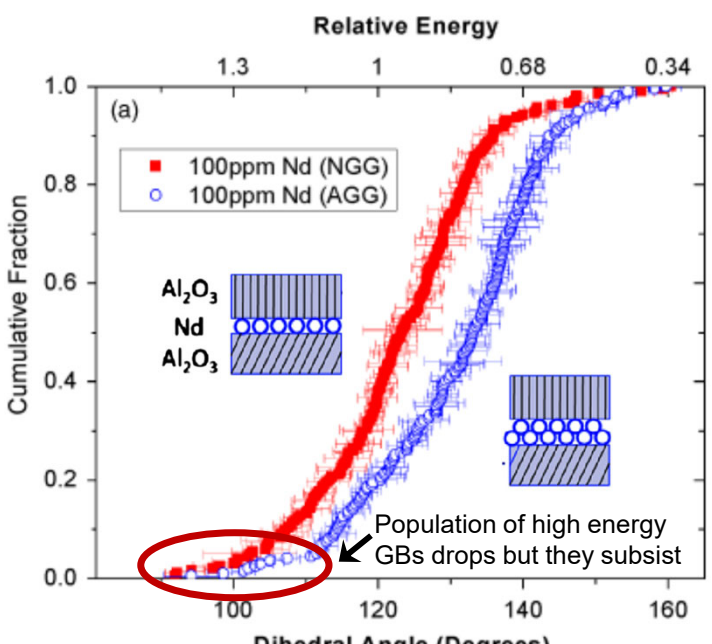

source: 10.1016/j.actamat.2013.07.037

Complexion transition phase diagrams

- Efforts ongoing to understand complexions to extend needed to generate **engineering diagrams** and relate to macro-properties
- Due to multi-dimensionality of complexion parameters (by opposition to phase transitions) **parameter space must be reduced** for plotting ➔ complexion diagrams only **stability guide**
- **In general:** Complexion transitions favored by **increasing temperature and dopant concentration**
- **Note:**
  Not all complexion types possible for all grain boundary characters ($\boldsymbol{R}$ and $\hat{\boldsymbol{n}}$) and e complexion depends on misorientation between sides of GB

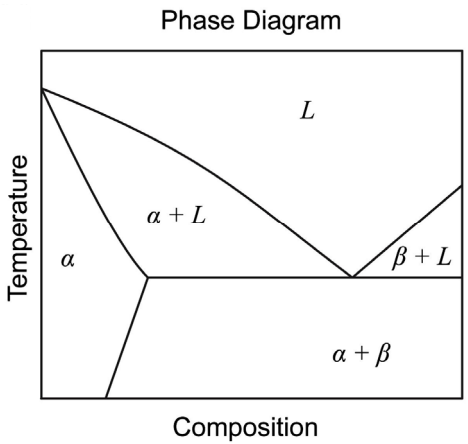

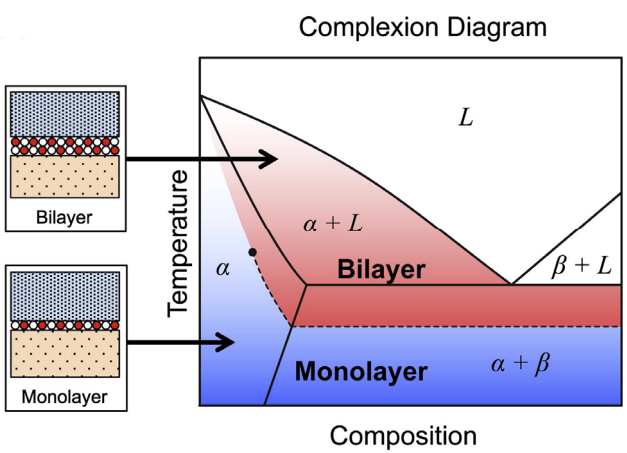

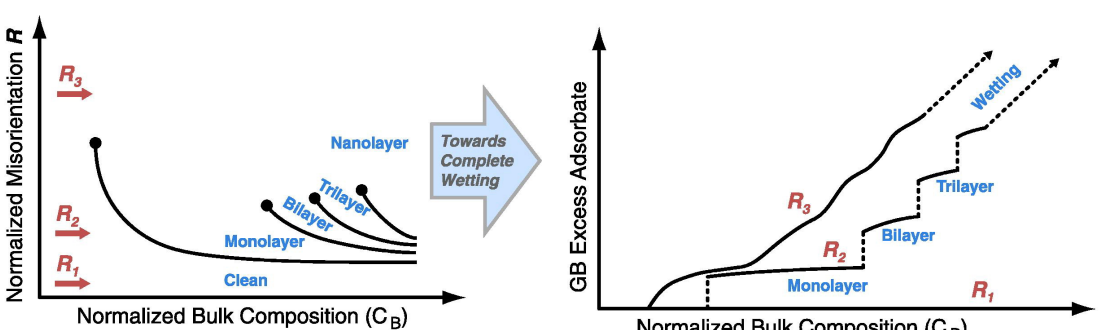

Basics about EBSD analysis

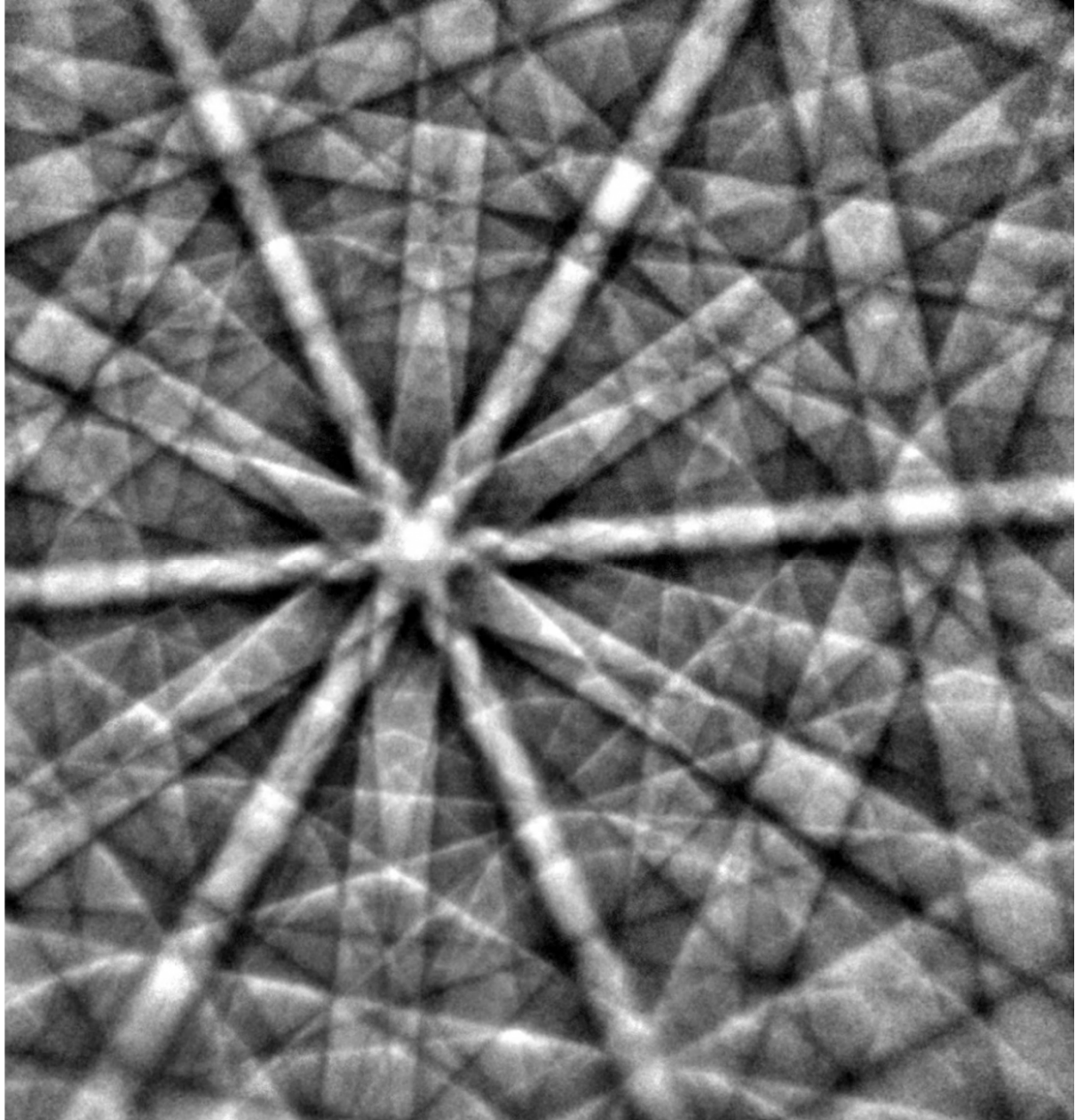

M. Stuer

EBSD basics

- **EBSD basics (short reminder)**:
  - For specific atomic planes electrons satisfy Bragg's law: $n\lambda = 2d \sin\theta$
    ➔ **Elastically scattered**, creating intense coherent wavefronts
  - Electrons undergo multiple diffuse elastic scattering interacting with periodic lattice
    ➔ **Kossel cone** formation
  - Interaction of Kossel cones with camera/phosphor
    ➔ **Kikucki lines** corresponding to family of hkl planes
  - Intersection of Kikuchi bands forms pattern **uniquely identifying crystal orientation**
    ➔ Possible to attribute **crystal orientation on a point-by-point basis ➔ EBSD maps**

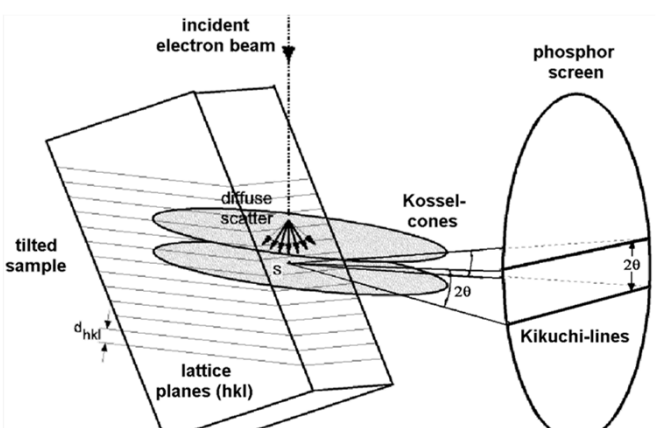

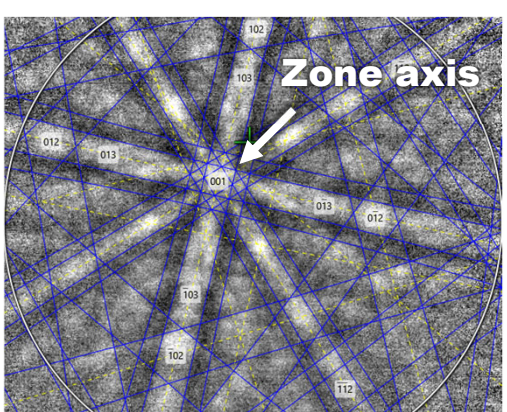

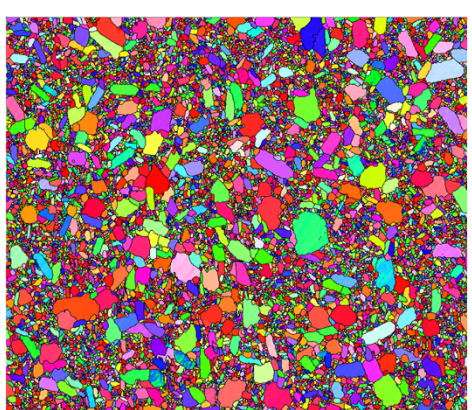

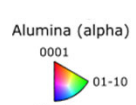

Additional background on EBSD basics

- For **10–30 keV electrons**, small Bragg angles (1–5°) lead to **nearly straight Kossel cone traces**
- On phosphor screen, Kossel cone pair from specific hkl lattice planes form Kikuchi lines, bounding the Kikuchi band
- Kikuchi **band width proportional to d-spacing** of the diffracting hkl lattice plane
- Indexing (Miller indices) done by comparing measured interplanar angles with known crystal structures (.cif file)
  ➔ Crystal structure has to be known!
- A consistently indexed triplet of lattice planes from different zones determines the crystal orientation
- Detected lattice plane positions have errors
  - ➔ Multiple potential crystal orientations possible
  - ➔ Different confidence and quality measures performed to find best (i.e. most likely) solution
- **High quality EBSD maps**
  = High quality sample preparation !

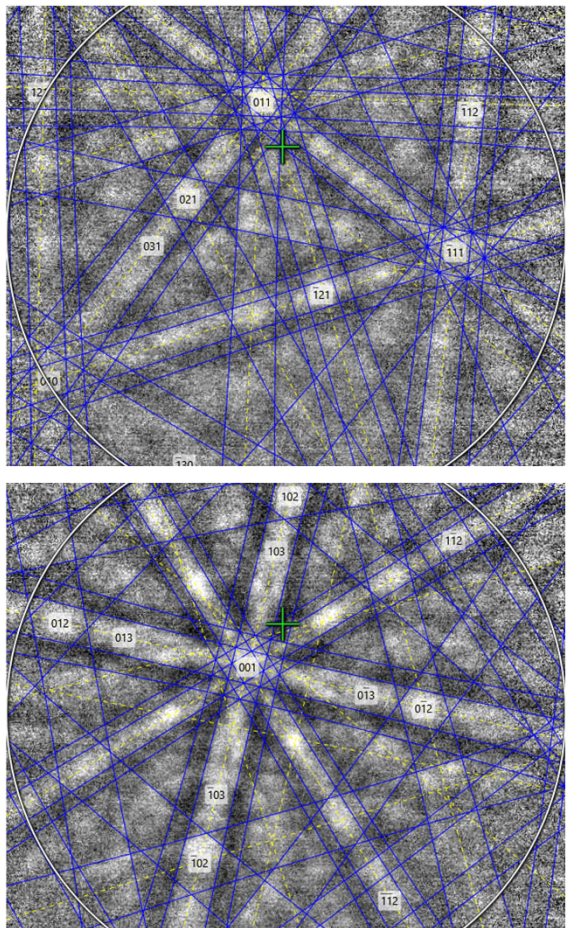

Orientation dependent Kikuchi patterns in a cubic crystal with automated line tracing and indexing in AZtec

Euler angles

- **Euler angles**
  set of **3 angles describing crystal orientation relative to a fixed reference frame**
  - Angles denoted as (ϕ_1, θ, ϕ_2) or (α, β, γ), depending on convention
- Euler angles typically define transformation angles **from sample to crystal reference** frame (i.e. coordinate system)
  - Orientation of each grain on EBSD map defined by its Euler angles
  - Rotation matrix $\boldsymbol{R} = \boldsymbol{R}_z(\phi_1)\boldsymbol{R}_x(\theta)\boldsymbol{R}_z(\phi_2)$
- **Note:**
  Reference frame can be freely chosen depending on analysis requirements
  - **Crystal reference frame**
    ➔ Grain boundary plane distribution
  - Bi-crystal reference plane
    ➔ Grain boundary character distribution

1st rotation: ϕ_1 around the Z-axis

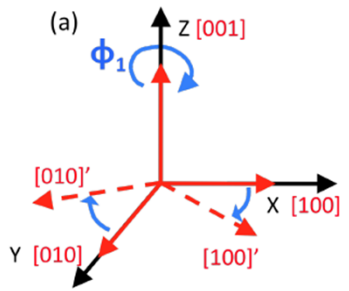

$$R_z(\phi_1) = \begin{bmatrix} \cos\phi_1 & -\sin\phi_1 & 0 \\ \sin\phi_1 & \cos\phi_1 & 0 \\ 0 & 0 & 1 \end{bmatrix}$$

2nd rotation: θ around the X-axis

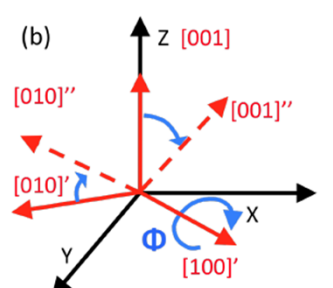

$$R_x(\theta) = \begin{bmatrix} 1 & 0 & 0 \\ 0 & \cos\theta & -\sin\theta \\ 0 & \sin\theta & \cos\theta \end{bmatrix}$$

3rd rotation: ϕ_2 around the Z-axis

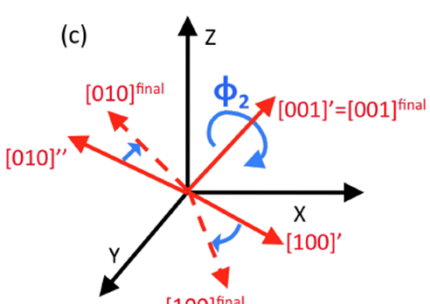

$$R_z(\phi_2) = \begin{bmatrix} \cos\phi_2 & -\sin\phi_2 & 0 \\ \sin\phi_2 & \cos\phi_2 & 0 \\ 0 & 0 & 1 \end{bmatrix}$$

EBSD basics

Stereological projections – Construction principle

- **Stereographic projection**
  Maps lattice directions and plane normals from a sphere onto an equatorial plane, preserving angular relationships
- **Construction** of stereographic projection
  - Position **crystal at the center** of the pole sphere
  - Determine the **intersections** of lattice directions or plane normals **with the pole sphere**
  - **Connect each intersection point to the opposite pole** using straight lines
  - Stereographic projection is the **intersection** of those lines **with equatorial plane** of sphere

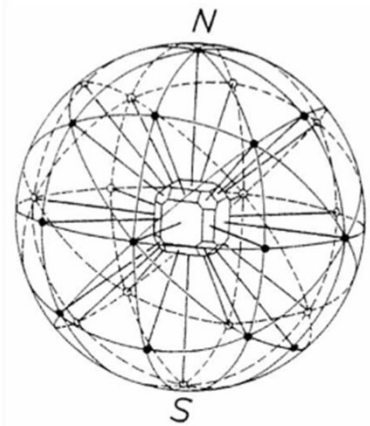

Cubic crystal placed in the center

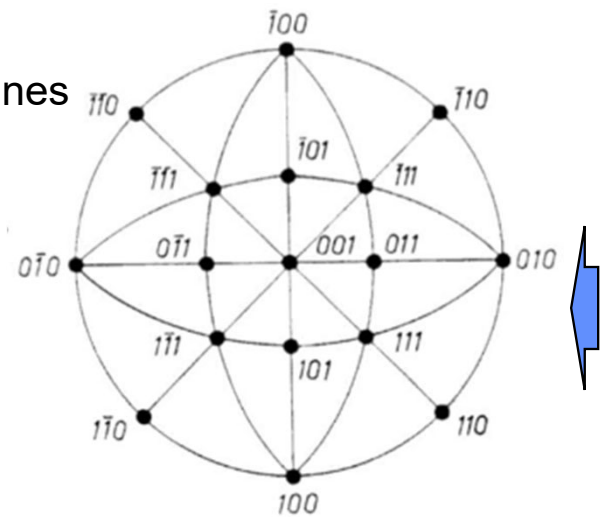

Stereographic projection of the upper hemisphere of (here) a cubic crystal

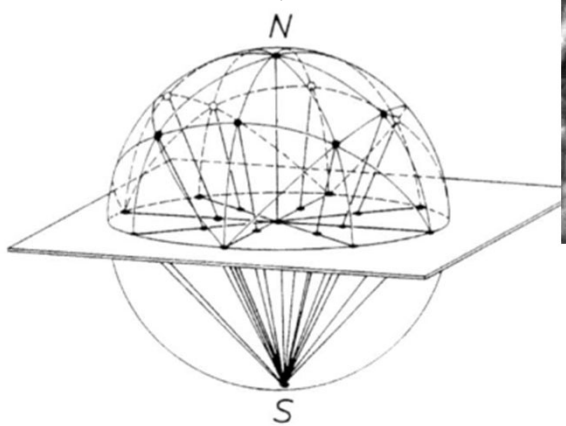

Projection onto the equatorial plane

Classical EBSD analysis: Pole figures

- Maps **distribution** of specific **crystallographic directions** (e.g. [111], [100], …) relative to **sample's** macroscopic **reference frame**
  - Axes (RD and TD) defined by sample orientation in reference frame
  - Used to represent texture

Defintion of Tilt and Rolling directions

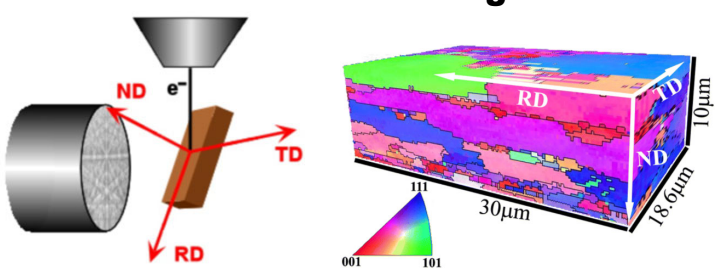

- **Note:**
  - **Point accumulation near pole figure center** may be apparent for randomly oriented samples due to **angular distortions**
  - When representing **large number of grains**, **pole overlap** on the pole figure obscures true orientation density ➔ **use contour lines**

Without preferred orientation/texture

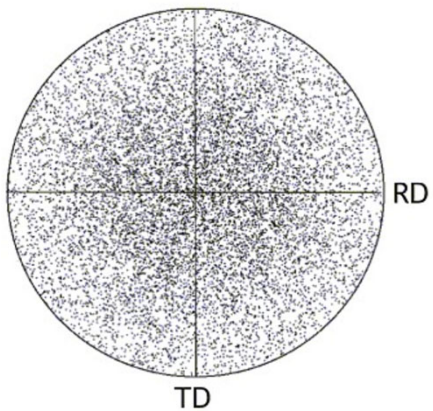

«cube» texture: preference for {100} orientations

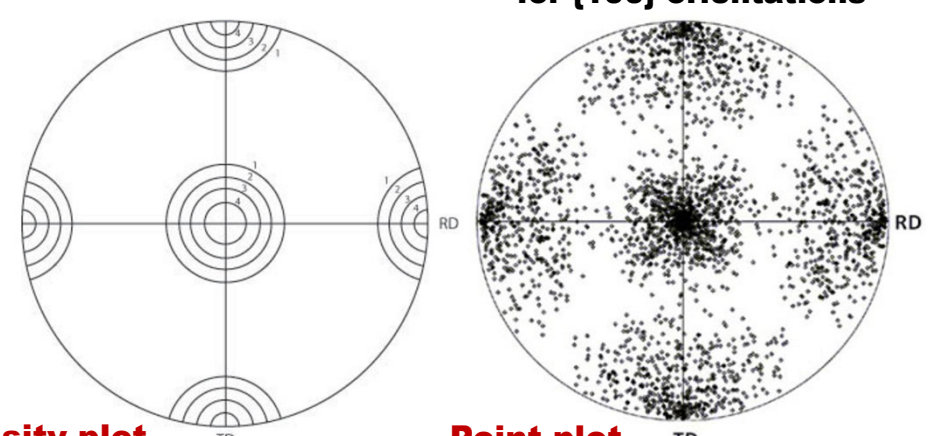

Density plot **Point plot**

EBSD basics

Classical EBSD analysis: Inverse pole figures

- Maps **relationship** between a specific **sample direction** (e.g. RD) **and crystal lattice**
  - Illustrated how crystal lattice is oriented relative to the macroscopic sample direction
  - Used to represent preferred grain alignment

- **Note:**
  - Shape and size of smallest domain containing all symmetrically non-equivalent directions depends on Laue group of respective crystal
  - Referred to as fundamental zone

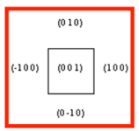

(001)[100]

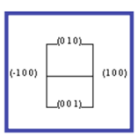

(011)[100]

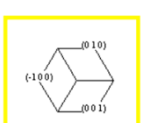

(-111)[211]

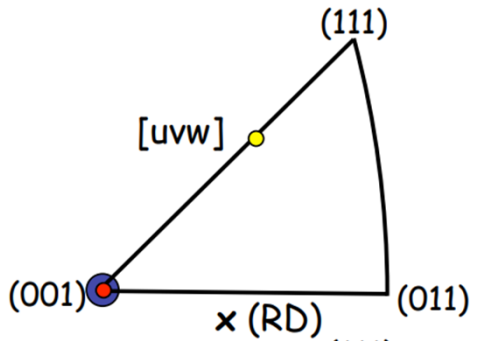

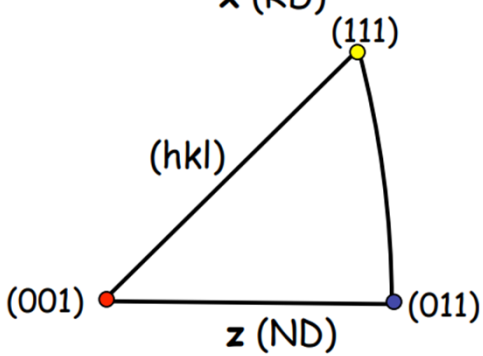

Fundamental zone of typical crystal systems

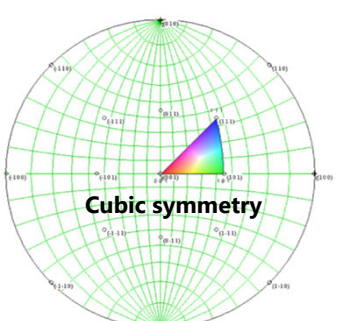

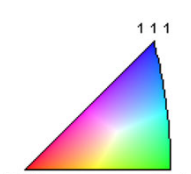

cubic

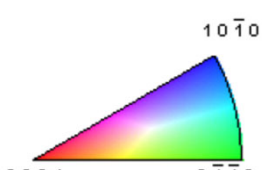

hexagonal

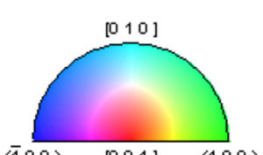

monoclinic

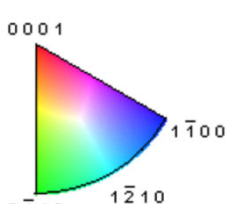

trigonal

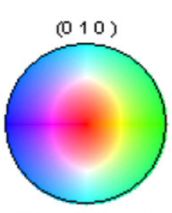

triclinic

Stereological projections – Case study

Effect of crystallographic orientation on transparency of PCA prepared using magnetic alignment and SPS

- EBSD map and the pole figure obtained from EBSD analysis of T plane perpendicular to magnetic field
- Most grains are red, orange and yellow indicating {0001} plane orientations with small angle deviations
  ➔ {0001} plane clearly aligned with T plane
- Also confirmed by transparency
  ➔ Alignment suppresses/reduces birefringence effect at grain boundaries
  ➔ Improved transparency confirms grain alignment along optical axis (e.g. {0001})

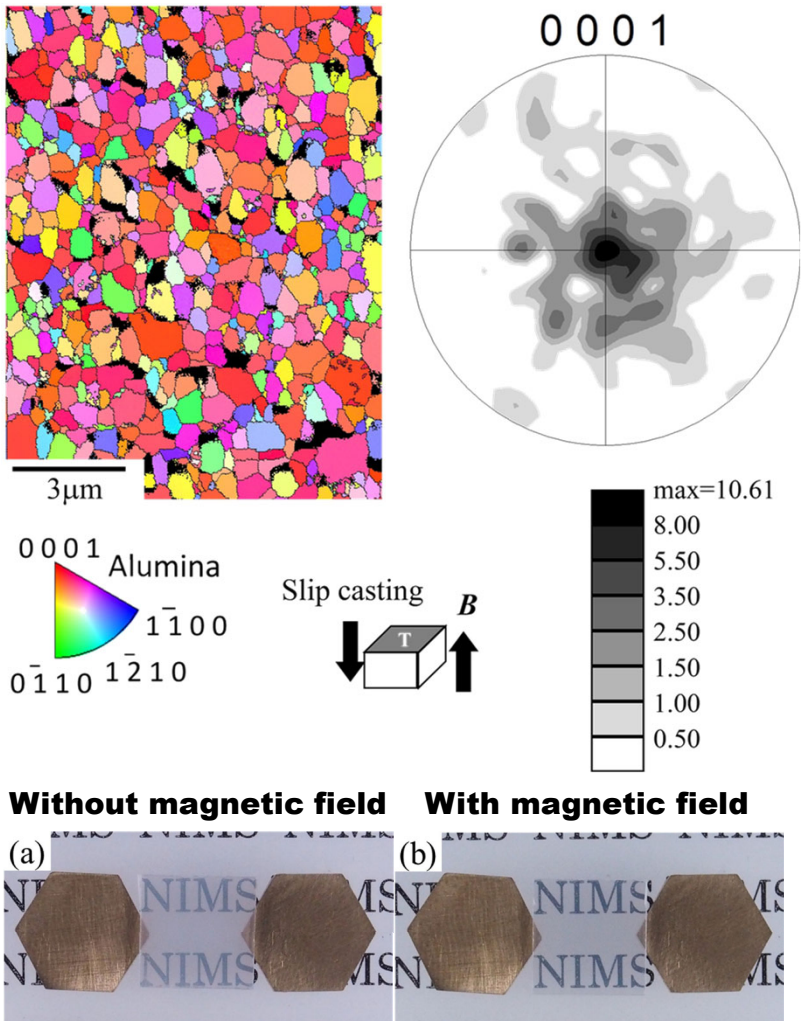

source: 10.1016/j.jeurceramsoc.2018.02.006

5-parameter GB character distribution - Stereological EBSD analysis

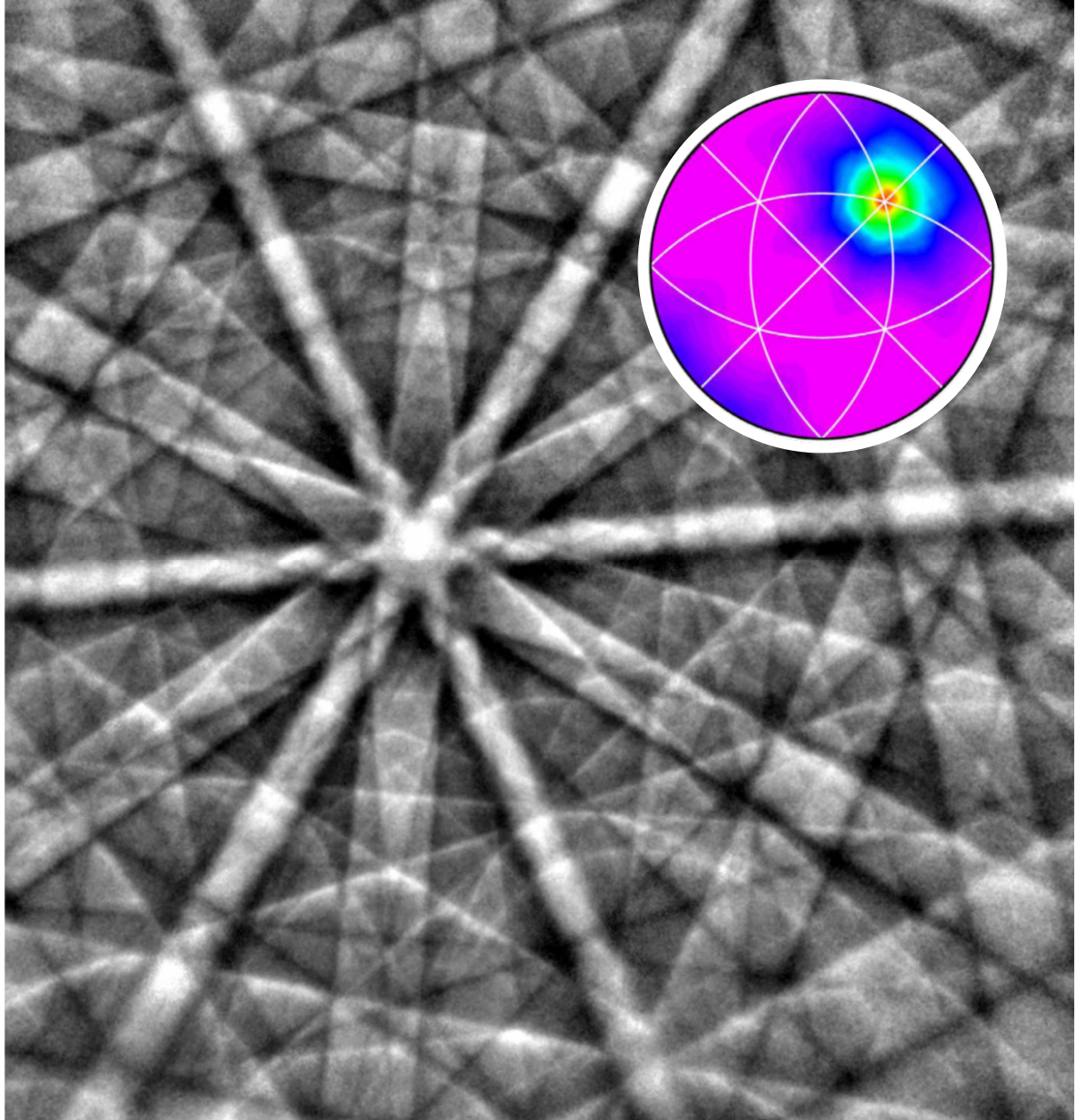

M. Stuer

Grain boundary characterization problem

- A grain boundary is defined by 5 macroscopic parameters:

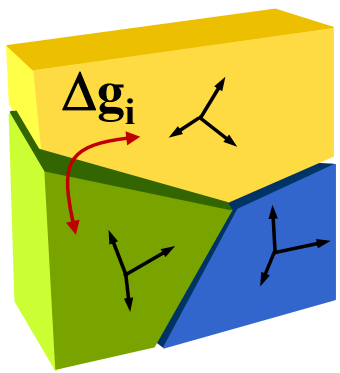

three to describe the misorientation

↳ **Directly computed from EBSD mapping data in commercial software**

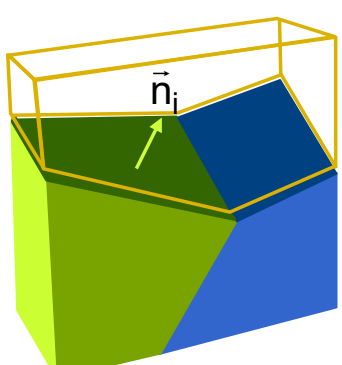

two for defining the GB plane orientation

↳ **?**

Stereological EBSD

Characterization approaches

- Two methods to determine the grain boundary plane:

1 FIB-EBSD-Nanotomography (3D EBSD technique)

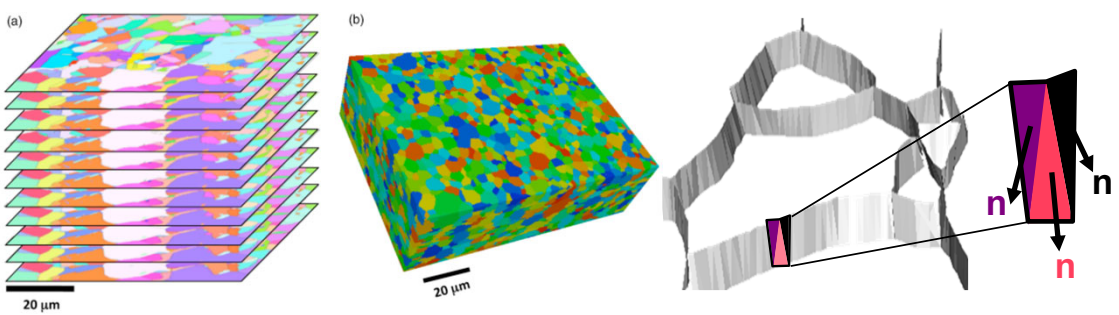

- Serial sectioning and EBSD acquisition
- Extract directly grain boundary character distribution from a specific sample area
  ➔ typically less available!

2 Stereological EBSD analysis

- More time-efficient and cost-effective than most 3D techniques
- Provides accurate estimates and offers statistical data from the entire sample
- But: Requires large datasets
  No direct 3D reconstruction of specific grains or grain boundaries

Stereological EBSD

Stereological analysis method

- **Stereology**
  Statistical method to estimate 3D structural properties from 2D cross-sections
- **Stereological EBSD analysis**
  Statistical method to determine grain boundary character distributions from 2-dimensional EBSD maps

GB detection → **Problem statement** → **GB trace analysis to define GB segments**

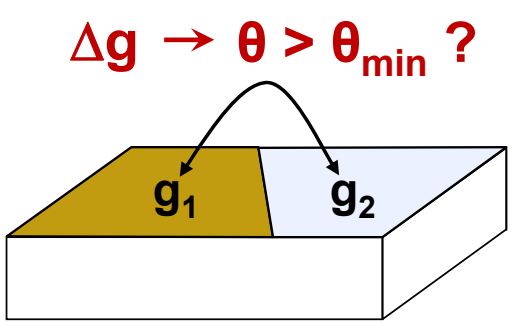

θ_{min} needed to avoid fake GB generation

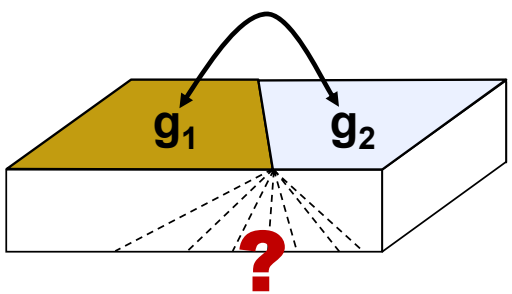

Missing:
GB plane orientation!

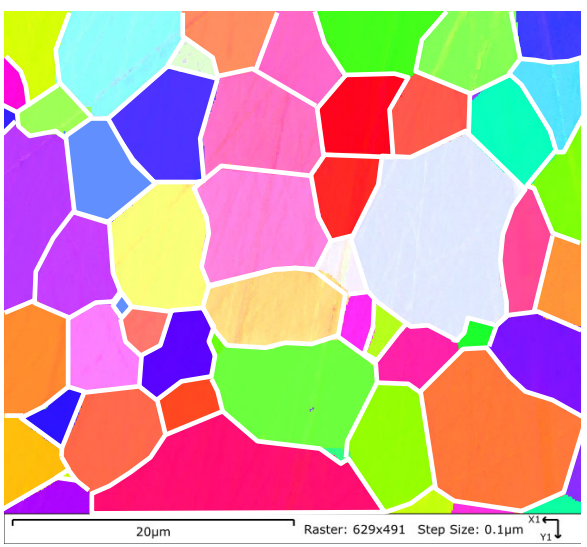

Stereological EBSD

Stereological analysis method

- From the GB trace analysis we know the zone axis of possible GB planes for each segment:

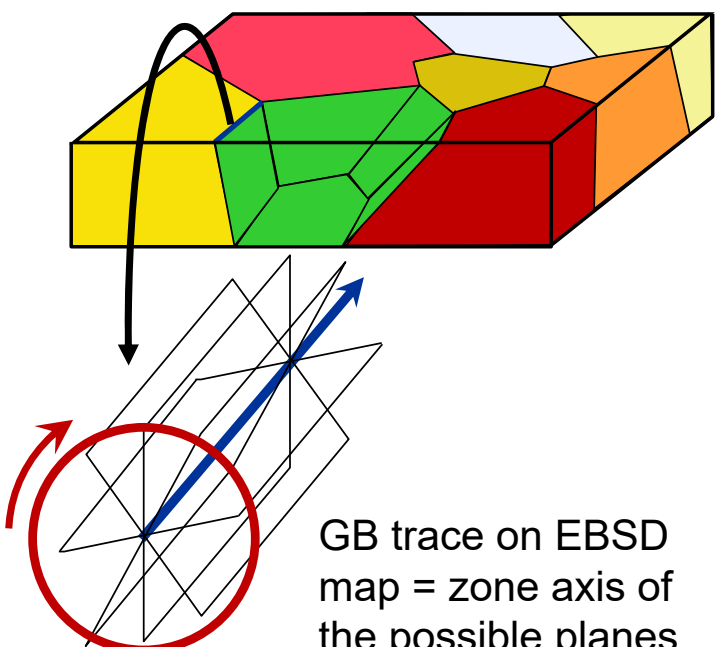

GB trace on EBSD map = zone axis of the possible planes

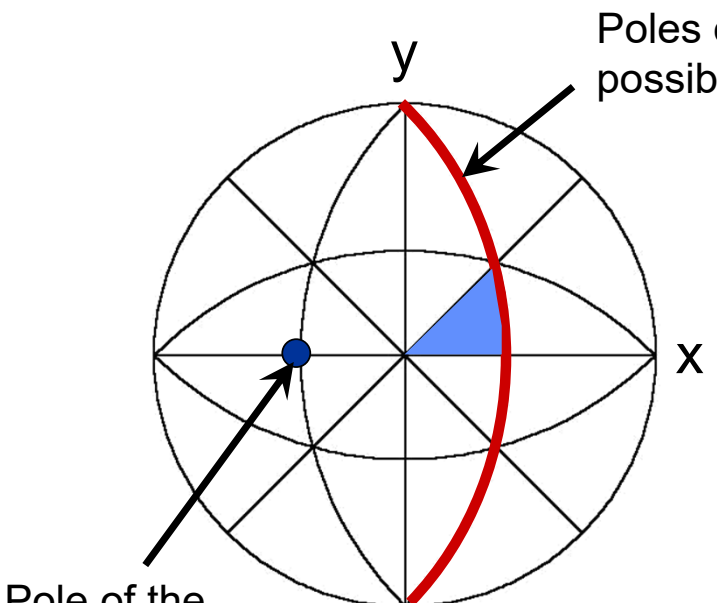

Poles of the possible GB planes

Pole of the GB trace

Stereological analysis method

- Superpose the poles of possible GB planes for GBs with a fixed Δg:

Grain boundary traces in sample reference frame

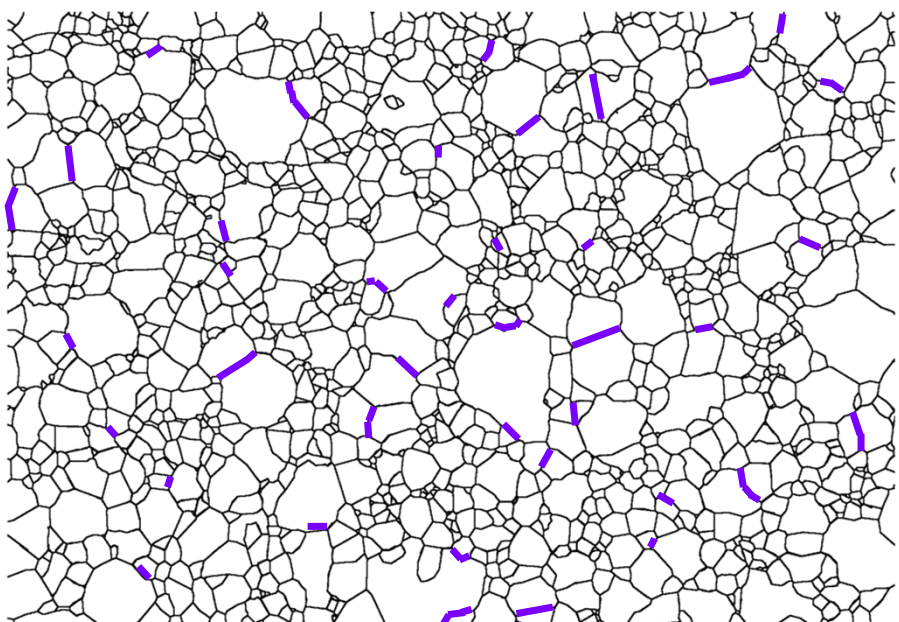

All planes in the zone of trace, in the misorientation frame (at a fixed Δg)

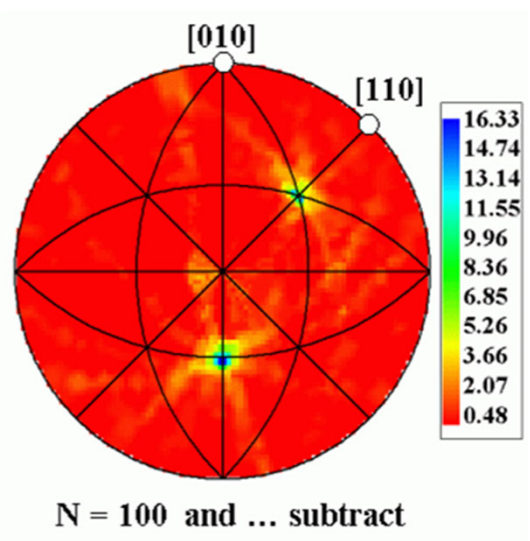

The **result** is a representation of the **true distribution of grain boundary planes at each Δg**

A continuous distribution requires roughly 2000 traces for each Δg

Stereological EBSD

Stereological analysis method – data requirements

- Max step size allowed for EBSD mapping function of grain size distribution
  ➔ ≥3 points per grain boundary required
- Amount of line segments required for statistically reliable analyses depends on crystal symmetry
  ➔ Higher symmetry reduces fundamental zone and thus required data amount

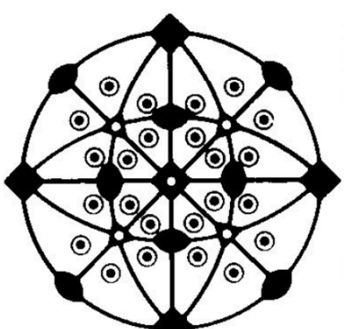

Cubic (m-3m)

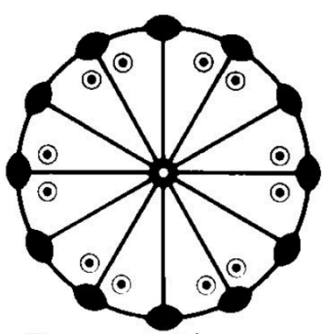

hexagonal (6/mmm)

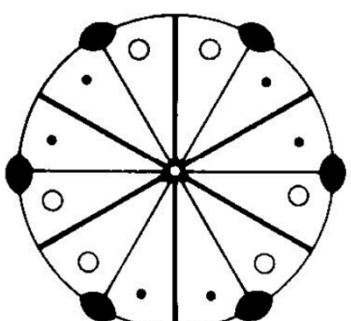

trigonal (-3m1)

Lattice symmetry	Line segments number requirement	
	$\lambda(\Delta g, n)$ mode	$\lambda(n)$ mode
cubic	0.5×10^4	0.2×10^4
hexagonal	20×10^4	0.5×10^4
tetragonal	45×10^4	1×10^4
trigonal	180×10^4	1×10^4

Grain boundary character distribution

Grain boundary plane distribution

Stereological EBSD

Stereological analysis method – GBCD representation

1-parameter GBCD	3-parameter GBCD
2-parameter GBCD	5-parameter GBCD

Misorientation angle distribution

- Represents grain boundary population as a function of minimum misorientation angle of each boundary
- max. possible misorientation is limited by crystal symmetry (example for trigonal 104.47°)

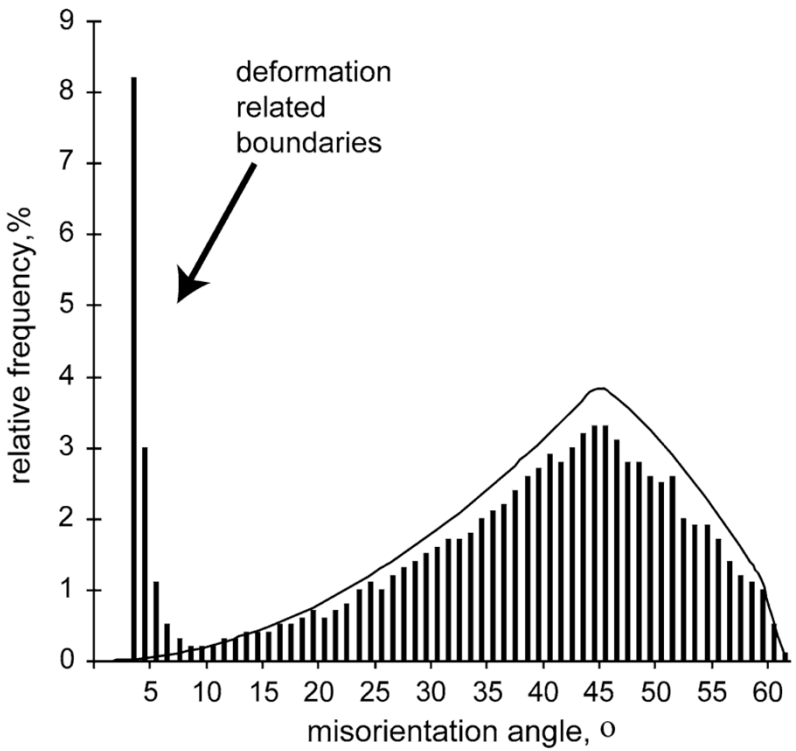

Misorientation angle distribution for NaCl after low strain deformation

Stereological analysis method – GBCD representation

1-parameter GBCD	3-parameter GBCD
2-parameter GBCD	5-parameter GBCD

Grain boundary plane distribution (GBPD)

- **Parameters:**
  - 1 normal of the grain boundary line segment
  - 1 angle of inclination of the grain boundary
- **Independent of misorientation angle**
- Typically plotted on stereograms looking down the [001] direction
- Plot: Full stereogram or fundamental zone

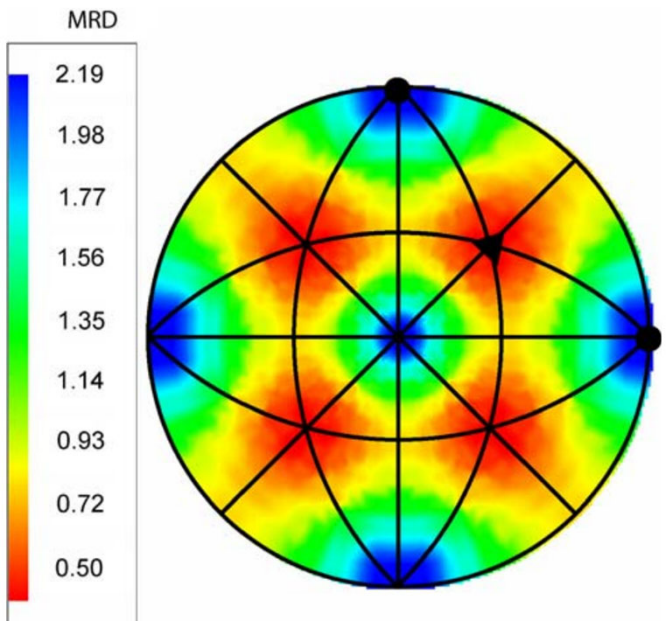

GBPD for all planes averaged over all misorientations in NaCl after low strain deformation

Stereological EBSD

Stereological analysis method – GBCD representation

1-parameter GBCD	**3-parameter GBCD**
2-parameter GBCD	5-parameter GBCD

Misorientation distribution function in the Rodrigues-Frank space

- **Parameters:**
  - 1 for the misorientation angle
  - 2 for the rotation axis

  between adjacent grains
- Plot: Sections of axis angle space
- Allows identifying around which crystal axis adjacent grains are preferentially rotated as a function of the angle (**independent of the grain boundary plane**)

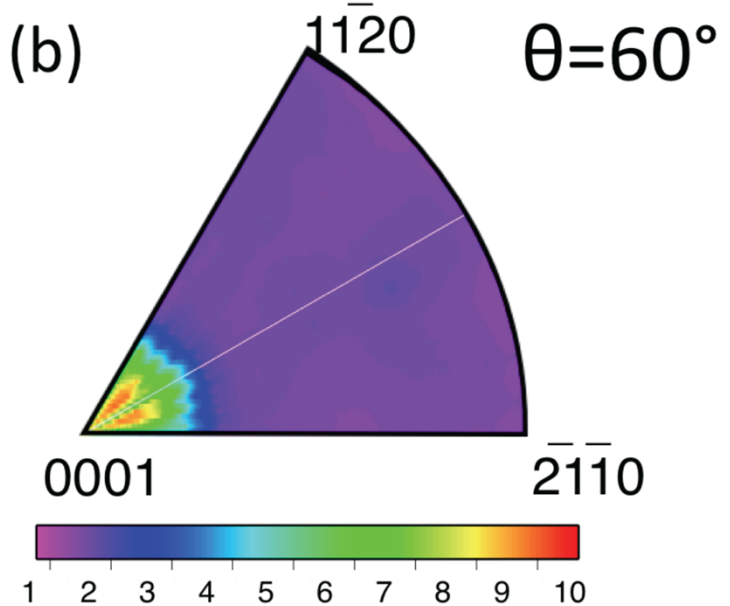

Section of the 3D misorientation distribution in alumina in axis-angle pair format

Stereological analysis method – GBCD representation

1-parameter GBCD	3-parameter GBCD
2-parameter GBCD	**5-parameter GBCD**

Grain boundary character distribution
(combining 2-parameter and 3-parameter GBCD)

- **Parameters:**
  - 3 for the misorientation
  - 2 for the grain boundary plane normal
  - ➔ Full geometric parameter description
- Plot: Always shown in full stereogram
- Plots distribution of grain boundary planes at fixed misorientation angle around specified axis
  - ➔ **Full geometric description of grain boundary**

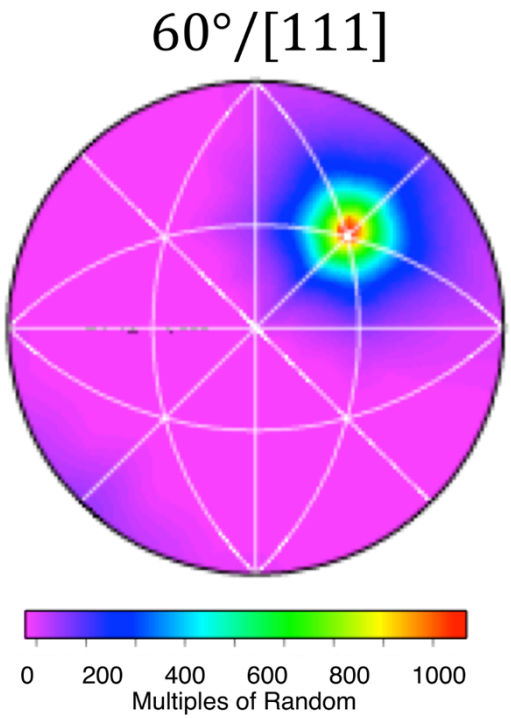

GBCD at a 60°/[111] misorientation (Σ3) for Ni

Effect of complexion transitions on grain boundary plane/character distribution

M. Stuer

Effect of dopants on GBPD

- Dopants change grain boundary energies which may directly affect grain boundary population

Example: MgO sintered for 15 hours to reach a thermodynamic "equilibrium"

- Especially Ca- and Y-doping lead to significant GBPD changes
- Ca-doping strongly favors occurrence of {100} planes
- Sr-doping has minor effect on GBPD

What is the role of complexion transitions ?

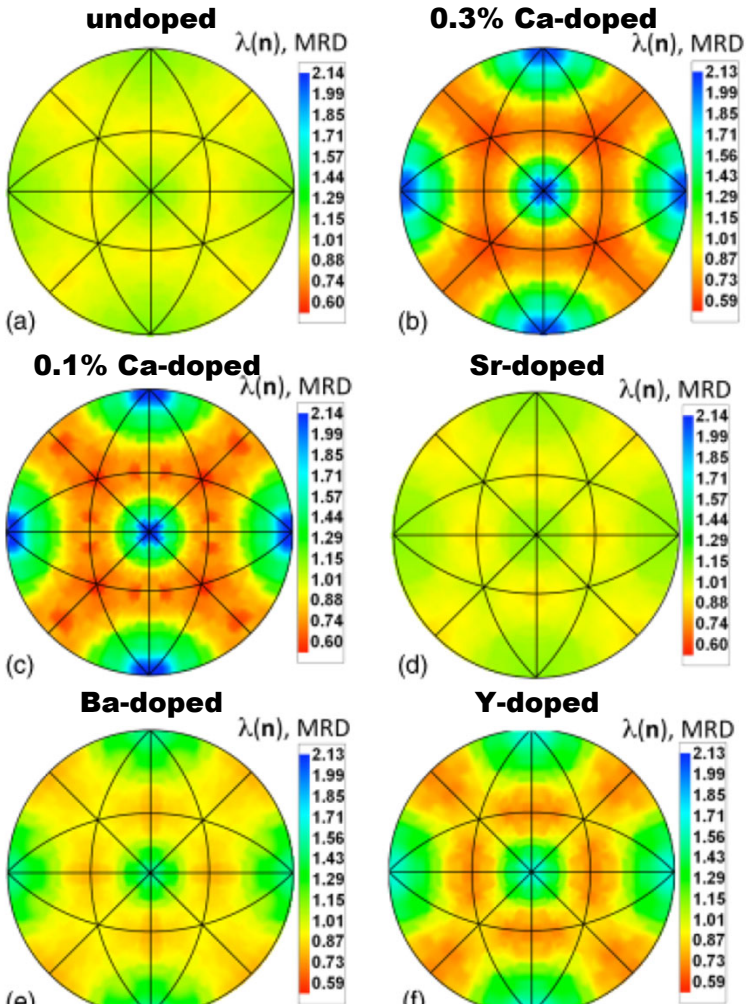

MgO samples sintered at 1600°C for 15h and thermally etched at 1400°C for 2-5h

Complexion effects

source: 10.1111/j.1551-2916.2011.04384.x

Effect of complexion transitions on GBPD

Example of Y-doped alumina

Sintering temperature
changed to prevent/trigger complexion transition!

	1400°C	1500°C	1600°C
Microstructure	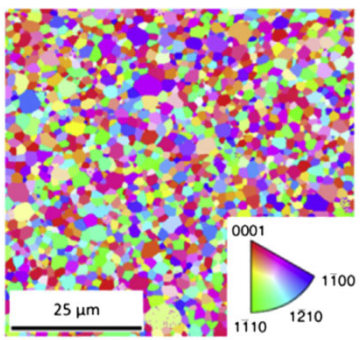	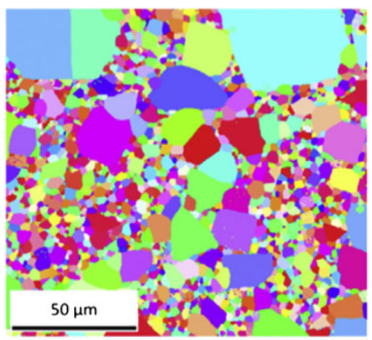	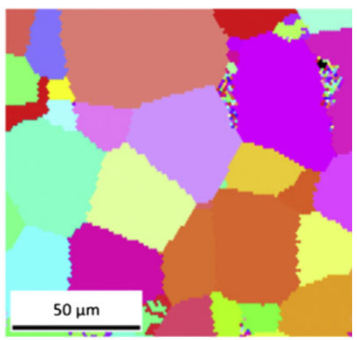
Stereological projection of grain boundary plane distribution	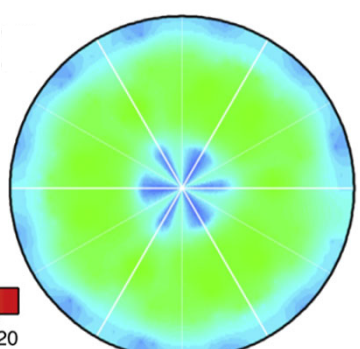	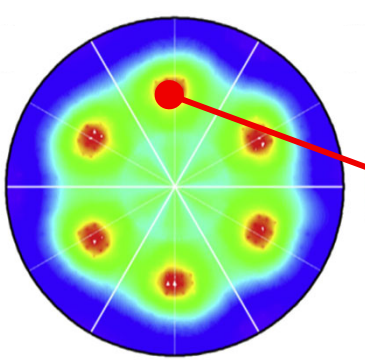	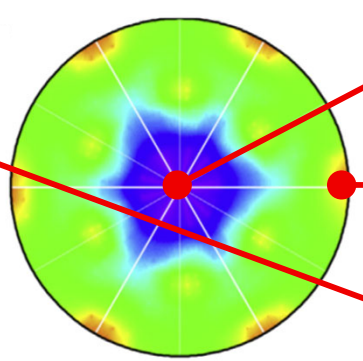

Grain growth needed to modify the grain boundary population!
Results suggest that R-planes in Y-doped alumina move faster!

Complexion effects

Effect of grain boundary energy on complexion transitions

Example of Y-doped alumina

- Complexion transitions reduce grain boundary energy
  ➔ previous slide: energy higher for $\{0001\}$ planes then for $\{11\bar{2}0\}$ or $\{1\bar{1}02\}$ planes
- Co-sintering of powder with single crystals to study grain boundary energy effect on complexion transitions

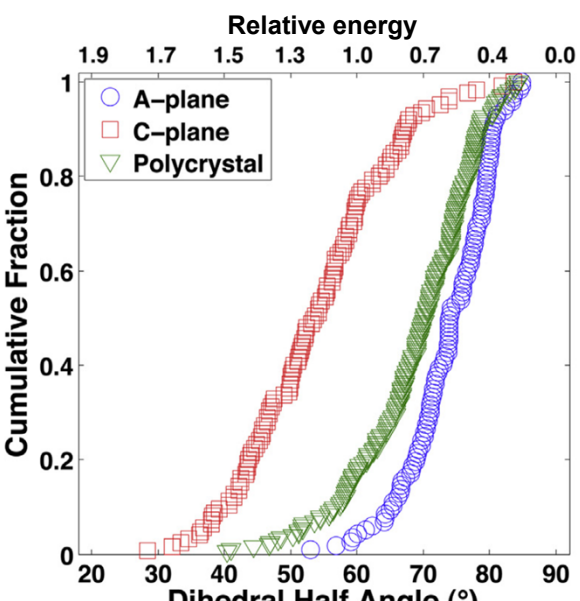

- After sintering at 1300°C (i.e. below complexion transition T°)
  - No microstructural difference between C- and A-plane interface
  - Average grain boundary energies higher for C- then A-plane interface or random distribution (i.e. polycrystal bulk)

After sintering below complexion transition T°

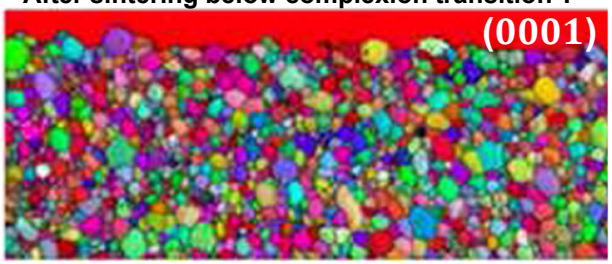

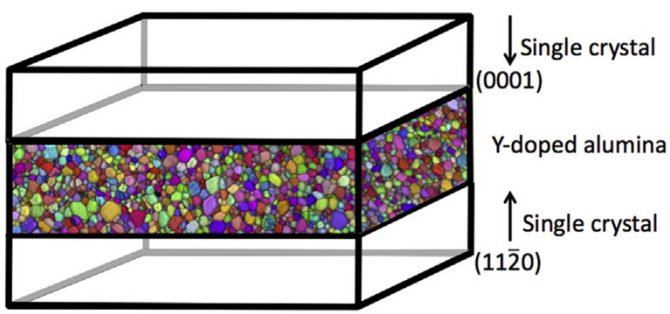

After sintering below complexion transition T°

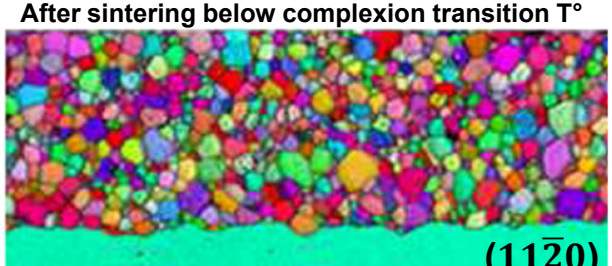

Complexion effects

source: 10.1016/j.scriptamat.2014.06.016

Effect of grain boundary energy on complexion transitions

Example of Y-doped alumina

- After complexion transition average grain boundary energy decreases at both interfaces but ranges appear to remain significantly similar. Two explanations:
  - ➔ High energy GBs form during grain growth
  - ➔ Complexion transitions occur by nucleation-growth
- Significantly larger grains at C-planes which can be due to:
  - Complexion transitions occurring at lower T°
  - Complexion transitions have lower nucleation energy barrier
- Interface moved further into the single crystal in C-plane compared to A-plane
  - ➔ mobility or growth time difference

Complexion transitions more likely to occur at high energy GBs

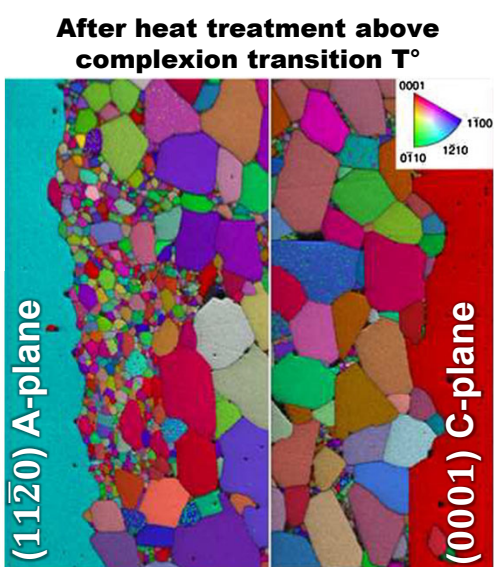

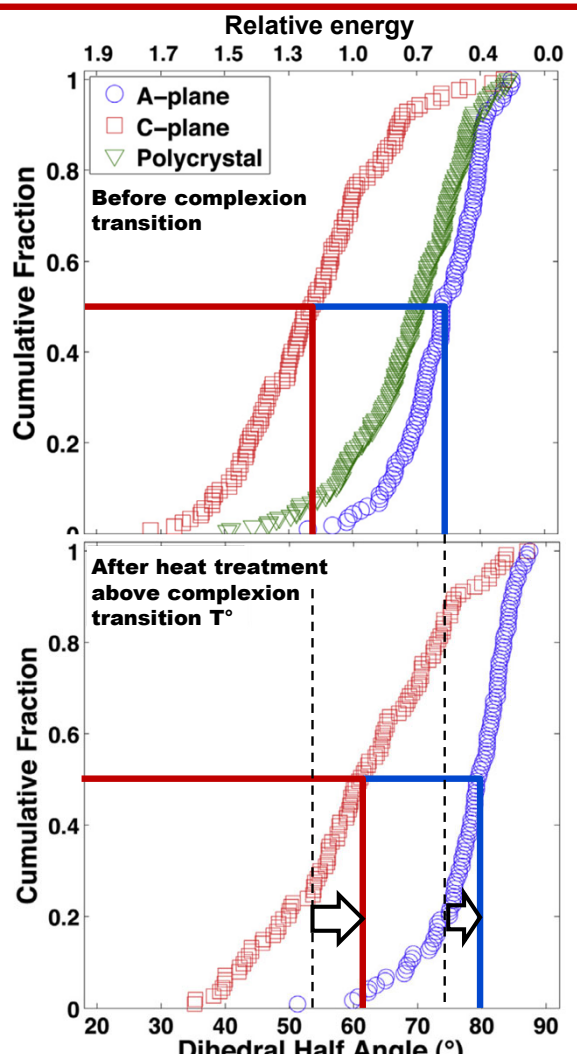

Complexion effects

source: 10.1016/j.scriptamat.2014.06.016

Effect of co-doping on GBPD

Example of Y- and La-codoped alumina

- Co-doping may (not a rule) allow combining effects on GBPD from single-doping

All samples sintered at 1500°C

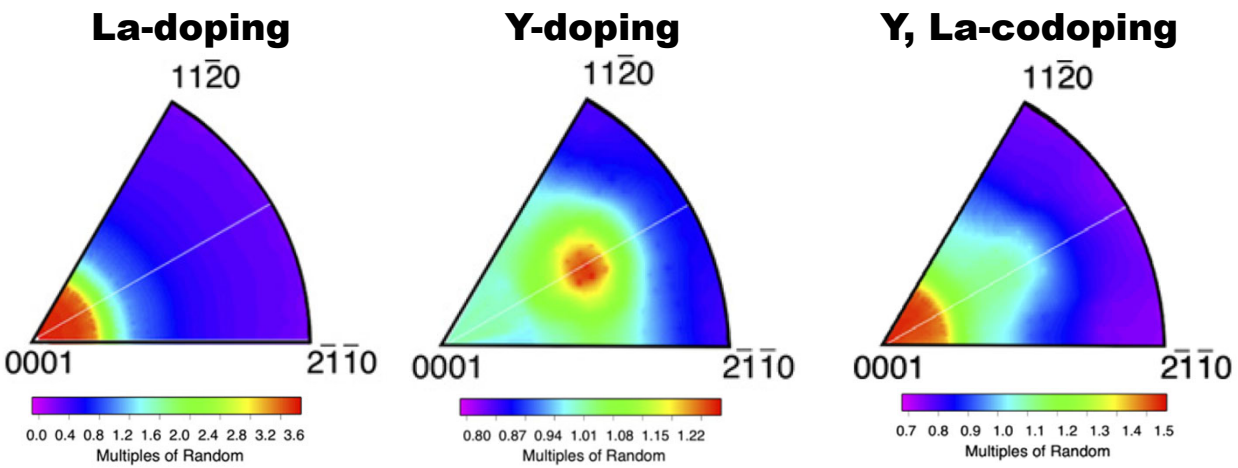

- Y-/La-codoping shows a preference for $\{0001\}$ and $\{1\bar{1}02\}$ oriented grain boundaries, whereby La-doping has a preference for $\{0001\}$ and Y-doping (at this temperature = transient) has a preference for $\{1\bar{1}02\}$

source: 10.1111/jace.12669

Final remarks

- Grain boundary engineering including complexions and complexion transitions is a new approach in advanced microstructure engineering
- It is not excluded that complexion transitions occur without affecting GB mobility but leading to other discontinuous property changes
- How to control grain boundary population and complexions in real systems
  - Particle crystal orientation alignment
    - ➔ use of anisometric particles (e.g. shear),
    - ➔ use of external forces during colloidal processing with anisotropic particles (e.g. magnetic alignment)
  - Use of adapted particle size to allow reaching target grain size after complexion transition induced grain growth
  - Use of dopants and dopant mixtures, including doping levels (i.e. complexion transitions typically involve chemical (dopant adsorption to GB) changes)
  - Trigger/avoid complexion transitions during densification by using rapid sintering techniques
  - Use of pressure or other external forces (i.e. complexion transitions obey thermodynamic laws)

source: 10.1111/jace.12669

The end

- **Summary**
  - Complexion and complexion transitions in grain boundaries
  - Type of complexion transitions and (non-)congruency thereof
  - Basics about EBSD
  - Stereological EBSD analysis to determine GBPD and GBCD
  - Effects of complexion transition on GBPD and GBCD towards advanced grain boundary engineering
- **Questions**